International Journal for Housing Science and Its Applications
Publish August 6, 2025. Volume 46, Issue 3 Pages 8570-8581

https,//doi.org/10.70517/ijhsa463732

Key factors influencing the phosphorus and sulfur cycles in soil mineral ions and microorganisms: A study based on principal component regression analysis

Lanxin Tang[1,*]
[1] School of Geographical Sciences, China West Normal University, Nanchong, Sichuan, 637002, China
Corresponding authors: (e-mail: lanxincwnu@163.com).

Abstract Soil mineral ions and microorganisms can convert easily degradable organic phosphorus and sulfur into more stable forms through processes such as adsorption, encapsulation, aggregation, redox reactions, and polymerization. This study selected rice field soil from Shenbei New District, Shenyang City, Liaoning Province, which has been continuously cultivated for many years, as the research object. Specific experimental procedures were established, and component analysis and adsorption kinetics calculations were performed on the samples. Based on this, to explore the impact of soil mineral ions and microorganisms on phosphorus-sulfur cycling, this study combined principal component analysis with regression analysis to construct a PCR model for validation. The results indicate that mineral ion complexes in soil enhance phosphorus adsorption, thereby facilitating soil phosphorus cycling, and that phosphorus-sulfur cycling exhibits certain differences across different soil types. The relative importance of soil mineral ions on phosphorus-sulfur cycling reached 31.42%, and both soil mineral ions and microbial abundance exerted a significant positive influence on phosphorus-sulfur cycling ($P < 0.01$). Therefore, optimizing mineral ion and microbial content in soil can significantly enhance phosphorus-sulfur cycling efficiency and further improve soil fertility.

Index Terms soil mineral ions, microorganisms, phosphorus-sulfur cycling, principal component regression, adsorption kinetics

I. Introduction

As the population continues to grow and technology continues to advance, land use and agricultural production methods have also evolved. However, this has also led to a series of environmental issues, including agricultural non-point source pollution, damage to terrestrial ecosystems, and reduced efficiency in carbon and nitrogen cycles [1]-[3]. Among these, nutrient cycling is a key area of focus in environmental science for addressing these issues, with the cycling of nutrients such as phosphorus and sulfur being a central component.

Nutrient cycling refers to the continuous reuse of nutrients such as phosphorus and sulfur, which are fixed in the soil, under the influence of biological and non-biological factors [4]. Phosphorus cycling primarily includes organic phosphorus mineralization, inorganic phosphorus mineralization, inorganic phosphorus synthesis, and inorganic phosphorus solubilization processes, while sulfur cycling primarily includes sulfuric acid oxidation, reduction, mineralization, and fixation processes [5], [6]. Nutrient cycles encompass both biological cycles (such as microbial activity) and non-biological cycles (such as element release, migration, adsorption, desorption, weathering, and precipitation). The entire cycle process can be divided into several aspects: plant absorption and utilization of phosphorus and sulfur; decomposition of organic matter within organisms and the cycling of decomposition products; transformation of inorganic nutrients in soil; and the redistribution and utilization of nutrients in material interactions [7]-[10]. The interconnections between these processes are extremely complex. The absorption and utilization of nutrients such as phosphorus and sulfur are highly dependent on the physical and chemical environment of the soil and the combined action of microorganisms. Mineral ions in the soil, such as calcium ions and nitrate ions, are closely related to phosphorus and sulfur cycles, regulating phosphorus and sulfur transformations through adsorption and desorption processes [11], [12]. In soil, microbial decomposition of organic and inorganic matter can directly or indirectly influence the cycling of nutrients like phosphorus and sulfur, such as by affecting phosphorus and sulfur metabolism, organic matter degradation, and phosphorus loss [13]-[15]. The quantitative relationships within organic matter also influence the biological cycling of nutrients like phosphorus and sulfur [16].

Carbonate ions belong to soil mineral ions. Literature [17] analyzed the impact of carbonates on phosphorus cycling, primarily through their conversion into organic carbon for microbial utilization. Extracellular calcium-phosphorus phase precipitation regulates phosphorus transport and promotes phosphorus cycling during

bioturbation and biomineralization. However, microorganisms adsorb phosphorus from the soil environment onto themselves, reducing phosphorus levels in the soil. Literature [18] reviews the role of soluble phosphorus-solubilizing microorganisms in the conversion of phosphates and soil phosphorus cycling. These microorganisms can regulate phosphorus forms and phosphate content, mineralize organic phosphorus, and solubilize inorganic phosphorus, thereby influencing soil phosphorus cycling. Literature [19] used Mantel and correlation analysis to conclude that the content of total organic carbon, total nitrogen, zinc, and cadmium in abandoned lead-zinc mine soils are the primary factors influencing carbon and phosphorus cycles.

In sulfur cycling, literature [20] highlights that halophilic microorganisms in desert soils are key species involved in sulfur cycling, while nitrate constrains the ecological networks of most sulfur genes in sulfur cycling. Literature [21] mentions that microorganisms mediate the conversion of organic sulfur to inorganic sulfur, i.e., the mineralization process, while some microorganisms decompose hydrogen sulfide from organic sulfur substrates in anaerobic environments. Additionally, in aerobic environments, reduced inorganic sulfur compounds are oxidized by some microorganisms, leading to stable redox states that influence sulfur cycling. Literature [22] found through functional gene array analysis that functional genes related to polyphosphate degradation and sulfite reduction in biological soil crust serve as the primary structural components of the phosphorus and sulfur cycles, respectively. Over a 61-year succession of biological soil crust, microbial metabolic activities related to phosphorus and sulfur cycles were stimulated. However, the key factors influencing the impact of soil mineral ions and microorganisms on phosphorus and sulfur cycles remain unclear.

Principal component regression (PCR) is an effective method for data processing and prediction. It reduces the dimensionality of data by projecting explanatory factors into principal component space, then uses regression models to generate predictive results [23]. PCR has advantages in reducing the number of factors and can effectively avoid certain types of multicollinearity. It also provides better predictive accuracy and more robust statistical models, and can effectively handle a large number of data factors, making it more convenient and accurate to capture key factors [24], [25].

Mineral-microbial interactions influence the migration and fate of phosphorus and sulfur, while soil mineral-driven phosphorus and sulfur cycling processes also affect the transformation and sequestration of organic matter. The experimental soil was collected from Shenbei New District, Shenyang City, Liaoning Province, and the experimental site was selected at the research and experimental base of Shenyang Agricultural University. Corresponding soil testing methods and procedures were designed. Adsorption kinetics were used to study the adsorption of phosphorus and sulfur elements by soil mineral ions. Principal component analysis and regression analysis were introduced to construct a principal component regression model to explore the specific effects of soil mineral ions and microorganisms on phosphorus and sulfur cycling, aiming to provide data support for improving soil fertility.

II. Materials and Methods

Soil mineral ions and microbial-derived organic matter influence phosphorus and sulfur material cycles and energy flow processes in soil, and their changes are often regulated by soil organisms (root systems and microorganisms) and mineral ions. A thorough analysis of the specific effects of soil mineral ions and microorganisms on phosphorus and sulfur cycles can help to further enhance soil fertility, thereby improving soil productivity.

II. A. Test Materials and Test Design

II. A. 1) Test materials

The test soil was collected from rice fields in Shenbei New District, Shenyang City, Liaoning Province, which have been continuously cultivated for many years. Shenbei New District is located in the mid-latitude zone of eastern Eurasia (123° 28′ E, 42° 06′ N). The region has a flat and open terrain with an average elevation of 60 meters. It has a temperate continental monsoon climate. In winter, it is influenced by a continental climate, resulting in dry and cold conditions with prevailing north and northwest winds. In summer, it is influenced by a marine climate, resulting in mild and rainy conditions with southerly and southwesterly winds. The spring and autumn seasons are short, with significant sandstorms. The monthly average temperature ranges from a high of 24.5°C to a low of -12.5°C. The average annual precipitation is 754.8 mm.

The experimental site is located at the S Agricultural University Research and Experiment Base, situated in the central area of the southern part of the Songliao Plain (123° 31′ E, 41° 48′ N). It has a temperate humid-semi-humid monsoon climate, with annual precipitation ranging from 620 to 820 mm, mostly concentrated in the summer (July to September). The annual average evaporation is 1,434.7 mm, with an average temperature of 7.1–8.2°C. The annual average sunshine duration is 2,443.8 hours, and the frost-free period is 150–185 days. The basic physical and chemical properties of the soil are shown in Table 1.

Table 1: Basic physical and chemical properties of the test soil

Organic carbon ($g \cdot kg^{-1}$)	Total nitrogen ($g \cdot kg^{-1}$)	Alkeline nitrogen ($mg \cdot kg^{-1}$)	Available phosphorus ($mg \cdot kg^{-1}$)
14.35	1.49	96.87	22.68
Available potassium ($mg \cdot kg^{-1}$)	Total phosphorus ($g \cdot kg^{-1}$)	Total sulfur ($g \cdot kg^{-1}$)	pH
125.79	3.46	19.62	6.53

II. A. 2) Experimental Design

(1) Experimental design

Four different soil types—black soil (BS), brown soil (OS), yellow-brown soil (YS), and red soil (LS)—were subjected to in situ soil (80 g) at different energy gradients (30, 60, 90, 150, 300 J/mL). The number of viable cells, as well as the mass fractions and organic matter concentrations of the components, were compared. A control group was established by adding sodium hexametaphosphate to the particle size fraction treatment to assess the optimal energy level.

After ultrasonication, the samples were divided into an ultrasonicated mixed solution (E1 group) and an ultrasonicated mixed solution screened for particle size fractionation (E2 group). Active microbial DNA from the E1 group was extracted, PCR amplified, and 16S rRNA sequenced using the propidium bromide (PMA) method to determine the effects of ultrasonication at different gradients on microbial communities. PMA and non-PMA treatments of soil were conducted according to methods described in existing relevant studies. The E2 group was grouped after sieving the mixture, and the mass fraction and organic matter concentration of each soil component (particles (POM) and mineral-associated organic matter (MAOM)) were determined.

After determining the appropriate ultrasonic energy, six different soil types—black soil, brown soil, yellow-brown soil, red soil, red-brown soil, and brick-red soil—were grouped, and basic physicochemical analyses of the POM and MAOM components were conducted, including pH, TN (total nitrogen), NH_4^+ (ammonium ions), NO_3^- (nitrate ions), P/S (phosphorus-to-sulfur ratio), iron-aluminum oxides, exchangeable calcium ions, iron-aluminum-bound carbon, calcium-bound carbon, and 16S rRNA sequencing.

(2) Soil grouping method

Based on existing soil grouping methods, the ultrasonic grouping method was further summarized and generalized. Twenty grams of in situ soil were weighed, and 50 mL of deionized water (soil-to-water mass ratio of 1:5) were added. The mixture was stirred using a vortex mixer, and soil aggregates were broken down using an ultrasonic disruptor. During ultrasonic treatment, the probe was positioned 0.5 cm below the liquid surface. An ice water bath is used to prevent temperature increases during ultrasonication that could affect soil microorganisms. Subsequently, using the optimal moisture sieving method, the sample is sieved through a 50 μm sieve and washed multiple times with deionized water. The residue on the sieve is POM, and the material passing through the sieve is MAOM after centrifugation. The suspension is centrifuged at 1000g for 20 minutes, with the temperature maintained at 5°C. After centrifugation, the supernatant is decanted, and both fractions are dried at 24°C.

Based on the Cotrufo grouping method, 0.5% sodium hexametaphosphate (HMP) solution and a small amount of glass beads are added to 10 g of soil sample and shaken for 20 hours to fully disperse the soil. The dispersed soil is then washed onto a 50 μm sieve, with the residue on the sieve representing POM, and the fraction passing through the sieve collected as MAOM. As in the previous step, the suspension is centrifuged at 1000g for 20 minutes at 5°C. After centrifugation, the supernatant is decanted, and the two fractions are dried at 24°C.

II. B.Sample measurement and data processing

II. B. 1) Sample determination

(1) Method for determining microbial carbon content. The method uses chloroform fumigation and K_2SO_4 extraction. Weigh two fresh soil samples, each weighing 6 g, into beakers, fumigate with chloroform for 24 hours, Additionally, an equal amount of soil is weighed as a non-fumigated control, kept in the dark for 24 hours, and extracted with 30 mL of 0.5 mol/L K_2SO_4 solution. The solution is filtered, and the phosphorus and sulfur content in the filtrate is determined using a TOC analyzer.

(2) Method for determining soluble organic phosphorus and sulfur. Weigh 12 g of fresh soil, extract with 0.5 mol/L potassium sulfate solution, shake at 300 rpm for 20 minutes, centrifuge, and filter through a 0.4 μm microporous membrane. Use a TOC analyzer to determine the phosphorus and sulfur content in the filtrate.

(3) Determination method for particulate organic carbon and mineral-bound organic carbon. Weigh 12 g of dry soil sample sieved through a 3 mm sieve into a volumetric flask, add 60 mL of 6 g/L sodium hexametaphosphate solution. Shake at 150 rpm for 20 hours, then sieve through a 0.05 mm sieve. Wash the soil particles larger than 0.05 mm through an aluminum tray. Particulate organic carbon is the fraction larger than 0.05 mm, and mineral-

bound organic carbon is the fraction smaller than 0.05 mm. Dry the separated solution at 70°C, weigh the dried material, and then determine the phosphorus and sulfur content.

II. B. 2) Data processing

The adsorption amount Q_t (mg·g-1) of amino acid-type organic matter by minerals at time t and the adsorption capacity at adsorption equilibrium are calculated using the following formulas:

$$Q_t = (C_0 - C_t) \times V / m \tag{1}$$

$$Q_e = (C_0 - C_e) \times V / m \tag{2}$$

where C_0 is the initial concentration of organic matter, C_t is the concentration of organic matter at different reaction times, C_e is the concentration of organic matter at adsorption equilibrium, V is the volume of the solution, and m is the mass of the mineral.

Adsorption kinetics can be used to study the specific steps in the adsorption process. By fitting adsorption kinetics models, the adsorption mechanism can be analyzed, reflecting the adsorption rate of the adsorbate on the adsorbent. This study employs quasi-first-order kinetics models, quasi-second-order kinetics models, and particle internal diffusion models to fit the adsorption kinetics process. Quasi-first-order kinetics models are typically used to study the effects of solution concentration and adsorption amount on adsorption rate, primarily describing physical adsorption processes. The pseudo-second-order kinetic model is primarily used to study adsorption processes dominated by chemical adsorption mechanisms, providing a more accurate reflection of the adsorption mechanisms involved in the entire adsorption process. The expressions for the pseudo-first-order kinetic model and the pseudo-second-order kinetic model are as follows:

$$Q_t = Q_e(1 - e^{-K_1 \cdot t}) \tag{3}$$

$$Q_t = (Q_e^2 \times K_2 \times t) / (1 + Q_e \times K_2 \times t) \tag{4}$$

where Q_e is the adsorption capacity of organic matter on minerals at equilibrium, and K_1 and K_2 are the pseudo-first-order and pseudo-second-order kinetic adsorption coefficients, respectively.

To further investigate the rate-limiting step of the adsorption process, the adsorption kinetic data were fitted using a particle internal diffusion model. The formula is as follows:

$$Q_t = K_d \times t^{0.5} + C \tag{5}$$

where K_d is the particle internal diffusion rate constant, t is the adsorption time, and C is the boundary layer thickness constant, representing the effect of diffusion through bound water on adsorption kinetics.

II. C.Principal component regression statistical model

II. C. 1) Principal component analysis

Principal Component Analysis (PCA) uses dimension reduction techniques to transform multiple variables in the original dataset into a few composite indicators, preserving as much of the original data information as possible while ensuring that the variables are mutually independent. The computational steps for PCA are as follows:

(1) Data preprocessing. Before performing PCA, the original data must first be preprocessed, which includes data cleaning, missing value handling, and outlier handling. Outlier handling can be performed using statistical methods or visualization methods to identify and handle outliers, thereby avoiding their impact on the analysis results. That is:

$$Z = \frac{x - \mu}{\sigma} \tag{6}$$

Among them, μ is the mean vector of each feature, and σ is the standard deviation vector of each feature.

(2) Calculate the covariance matrix. Calculate the covariance matrix $\sum$ of the standardized data matrix Z. That is:

$$\sum = \frac{1}{n-1} Z^T Z \tag{7}$$

The covariance matrix $\sum$ describes the linear correlation between features and provides the basis for subsequent eigenvalue decomposition.

(3) Eigenvalue decomposition. Perform eigenvalue decomposition on the covariance matrix $\sum$ to obtain the eigenvalues λ_i and eigenvectors V_i. That is:

$$\sum V_i = \lambda_i V_i \tag{8}$$

Through eigenvalue decomposition, a series of eigenvalues and corresponding eigenvectors can be obtained.

(4) Select principal components. Arrange the eigenvalues in descending order and select the first k eigenvectors as the basis for the principal components. The number of principal components k can be determined based on the cumulative explained variance ratio. Generally, the first k principal components that achieve a cumulative explained variance of 80%-90% are selected. That is:

$$\text{Cumulative interpretation variance ratio} = \frac{\sum_{i=1}^{k} \lambda_i}{\sum_{i=1}^{p} \lambda_i} \tag{9}$$

(5) Calculate the principal components. Using the selected principal components and their corresponding feature vectors, calculate the scores of the original data on each principal component, which reflects the position information of the original data in the low-dimensional space after dimensionality reduction. Project the standardized data Z onto the selected principal component basis to obtain the low-dimensional data representation Y. That is:

$$Y = ZV_k \tag{10}$$

Among them, V_k is the matrix formed by the first k eigenvectors.

II. C. 2) PCR model

PCA achieves dimensionality reduction by transforming m highly correlated original variables into $A(A \square m)$ mutually independent principal components (also known as principal components or latent variables). This process not only retains most of the variation information in the data but also reduces the dimensionality of the data, thereby alleviating multicollinearity issues and improving the robustness and predictive power of regression models. For an $(n \times m)$-dimensional data matrix X, the PCA model is generally represented as follows:

$$X = \sum_{a=1}^{A} t_a p_a + E \tag{11}$$

where $t_a(n \times 1)$ and $p_a(1 \times m)$ are the score vectors and load vectors corresponding to the a principal element. $E(n \times m)$ is the residual matrix of the PCA model, which contains $(m - A)$ unpreserved principal elements of the model. t_a and p_a are represented by the score matrix $T(n \times A)$ and the load matrix $P(m \times A)$, respectively, which can be recorded as:

$$X = TP^T + E \tag{12}$$

Through dimension reduction using the PCA model, the original data $X(n \times m)$ with collinearity is converted into a matrix of mutually independent principal component scores $T(n \times A)$. At this point, a principal component regression (PCR) model is established between the score matrix $T(n \times A)$ and the output data $Y(n \times k)$, thereby obtaining:

$$X = TP^T + E \tag{13}$$

$$Y = TB + F \tag{14}$$

Among them, $B(A \times k)$ is the coefficient matrix, which is estimated by the least squares method, that is:

$$B = (T^T T)^{-1} T^T Y \tag{15}$$

Since the equation contains structural information about the input data X, this information is present in the rows of the PCA model load matrix P. At this point, product design based on the principal component scores in the PCA model can transfer the structural information from historical data to the new input conditions x^{new}, thereby ensuring that x^{new} remains consistent with past input conditions. Therefore, the new input conditions x^{new} should satisfy:

$$x^{new} = t^{des} P^T \tag{16}$$

Among them, t^{des} is expressed as:

$$y^{des} = t^{des} B \tag{17}$$

It can be seen that in order to calculate x^{new}, it is necessary to first solve t^{des} and then reconstruct it. The calculation of t^{des} reduces the dimension of the unknown conditions from m to A, thereby reducing the computational complexity.

Since the product design problem has now been transformed into estimating A principal components from k output variables, the following three cases need to be considered when solving t^{des}:

(1) $k > A$: Solving t^{des} is equivalent to projecting from a high-dimensional (k) space to a low-dimensional (A) space, and its least squares solution can be calculated.

(2) $k = A$: In this case, t^{des} can be directly obtained by calculating the inverse of B.

(3) $k < A$: At this point, the data needs to be projected from the low-dimensional (k) space to the high-dimensional (A) space, which typically occurs when the rank of the input matrix X is much greater than the number of quality variables k.

For cases (1) and (2), t^{des} typically has a unique solution. However, for the underdetermined case (3), t^{des} has infinitely many solutions, consisting of general solutions and particular solutions. Here, we take the pseudoinverse of B as one of the particular solutions, denoted as:

$$t^{des} = y^{des} (B^T B)^{-1} B^T \tag{18}$$

At this point, the input conditions x^{new} for the new intermittent process product can be calculated as follows:

$$x^{Dew} = t^{des} P^T = y^{des} M^T \tag{19}$$

Among them, $M^T = (B^T B)^{-1} B^T P^T$.

III. Results and Analysis

Soil is the material foundation for plant survival, and the amount of organic carbon in the soil determines its fertility. To provide plants with good material conditions for growth and development, it's really important to increase the amount of organic microorganisms and mineral ions in the soil. Microorganisms and mineral ions aren't just essential nutrients for plant growth and development, but they also play a crucial role in fixing organic carbon in the soil.

III. A. Soil organic microbial content

III. A. 1) Soil organic carbon content

To effectively analyze the organic carbon content in different soils, this study collected three types of soils (BS, OS, YS, and LS) from the research and experimental base of S Agricultural University at three different time points (T1–T3). The organic carbon content of the four soil types was measured, and the results are shown in Figure 1. Different lowercase letters in the figure indicate significant differences between different soils at the same time period, while different uppercase letters indicate significant differences between different time periods for the same soil type ($P < 0.05$).

The SOC content of different soil types showed little variation across all time periods. The differences in SOC content between BS and OS soils at different time periods did not reach significant levels ($P > 0.05$). The SOC content of YS soil showed a decreasing trend across different periods, with significant differences observed between T2 and T3 ($P < 0.05$). The SOC content of LS soil exhibited an initial increase followed by a decrease across the entire period, with significant differences observed between T1 and T2 ($P < 0.05$). . Compared to BS soil, OS, YS, and LS soils showed varying degrees of increase in soil organic carbon content. At T1, YS soil significantly increased by 12.18%, 5.74%, and 4.98% compared to BS, OS, and YS soils, respectively, while no significant differences were

observed among BS, OS, and YS soils (P > 0.05). During the T2 period, YS soil showed significant increases of 10.05%, 9.48%, and 7.52% compared to BS, OS, and YS soils, respectively. However, no significant differences were observed among BS, OS, and YS soils (P > 0.05). In the T3 period, YS soil had the highest SOC content at 16.18 ± 2.42 g/kg. Compared with BS, OS, and YS soils, YS soil significantly increased organic carbon content by 18.03%, 8.74%, and 6.35%, respectively.

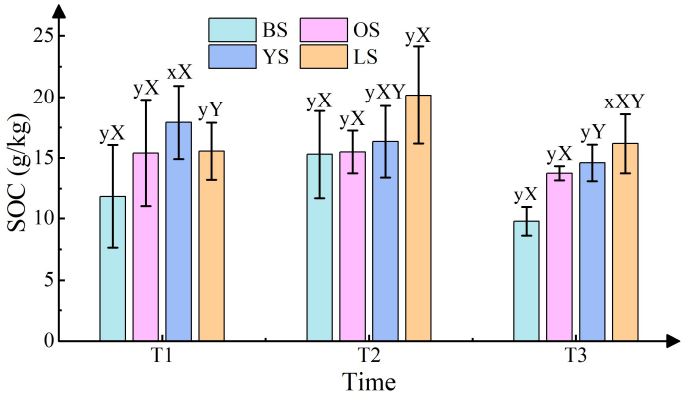

Figure 1: Soil organic carbon content

III. A. 2) Soil microbial biomass content

Figure 2 shows the carbon content of microbial biomass in different soils at different time periods. As shown in the figure, there are significant differences in MBC content among different soil types across different periods. BS and OS soils exhibit a decreasing trend in MBC content across all periods, while YS and LS soils show an initial increase followed by a decrease in MBC content across all periods. MBC content in all soil types remains relatively stable in T1 and T2, but drops sharply in T3. The differences between T1/T2 and T3 are statistically significant (P < 0.05). During the T1 period, compared with BS soil, the MBC content in OS, YS, and LS soils increased significantly by 19.15%, 30.08%, and 24.84%, respectively. However, there were no significant differences among OS, YS, and LS soils (P > 0.05). In the T2 phase, compared with BS and OS soils, the MBC content in YS and LS soils increased significantly by 68.75%, 42.13%, 54.08%, and 28.97%, respectively. In the T3 phase, the MBC content in OS, YS, and LS soils increased significantly by 24.09%, 67.93%, and 33.14%, respectively, compared with BS soil.

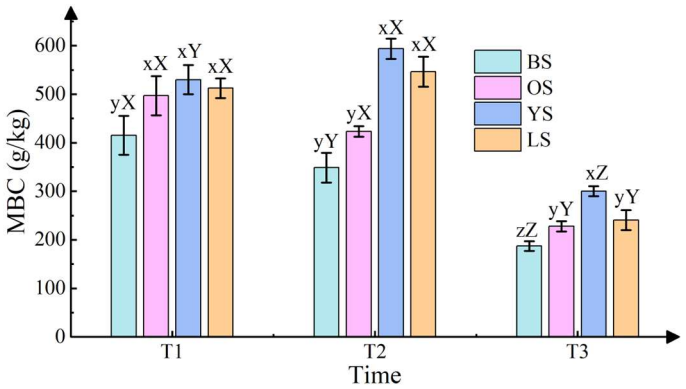

Figure 2: Soil microbial biomass content

III. B. Mineral ion adsorption and phosphorus-sulfur changes

III. B. 1) Changes in soil TN, AP, and TS

This study measured changes in soil total nitrogen (TN), available phosphorus (AP), and total sulfur (TS) in four different soil types. Four different soil types were selected for a 120-day cultivation period, and changes in TN, AP, and TS in the soil were tested, as shown in Figure 3, where Figures 3(a) to (c) represent the trends in TN, AP, and TS, respectively.

As shown in Figure 3(a), the TN levels of all soil types fluctuated between 0.78 and 1.39 g/kg. Over the 120-day incubation period, TN levels showed a decreasing trend. Both BS and YS soils followed a pattern where TN levels gradually decreased within the first 12 days of incubation, then increased between 12 and 48 days, reaching peaks

of 1.36 g/kg and 1.24 g/kg, respectively. From 48 to 72 days, TN decreased, and then stabilized by 120 days. In OS soil, TN decreased rapidly within 2 days and showed fluctuating changes as the incubation time increased. In LS soil, TN decreased within 6 days, reached a maximum of 1.19 g/kg between 36 and 48 days, and then decreased by 72 days. Within 72 days, compared with BS soil, TN in OS soil decreased significantly by 21.58%, while TN in YS and LS soils decreased by 7.37% and 9.51%, respectively. Within 120 days, compared with BS soil, TN in OS soil decreased significantly by 7.13%, while there was no significant difference in TN between YS and LS soils.

The level of total sulfur (TS) in soil depends on the content of organic matter and soil quality. The results of this study showed that the TS content of different soil types exhibited a segmented increase trend over the 120-day cultivation period, with increases occurring between 0–12 days and 72–106 days, while remaining relatively stable between 12–72 days (as shown in Figure 3(b)). Within 12 days, TS ranged from 60 to 115 mg/kg, with no significant differences between OS, YS, and LS soils compared to BS soil. Within 72 days, TS content changes were minimal across all soil types, fluctuating around ±8 mg/kg. Compared to BS soil, OS soil showed a significant increase of 6.48%, with OS soil significantly higher than YS and LS soils, while no significant differences were observed between YS and LS soils. Within 120 days, there were no significant differences between OS and YS soils, nor between LS and BS soils. The TS content of OS soil decreased by 9.43% compared to BS soil and by 10.21% compared to LS soil. Compared to BS and LS soils, the TS content of YS soil decreased by 13.47% and 13.98%, respectively.

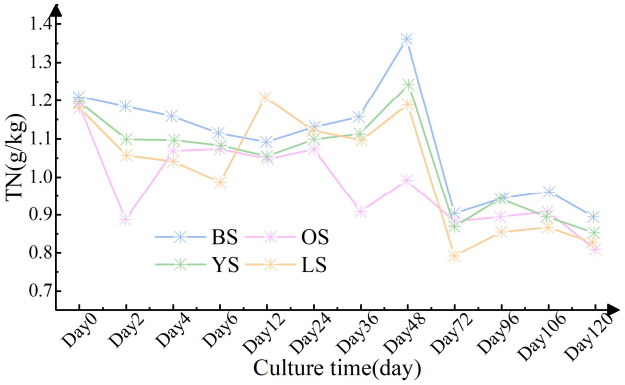

(a) TN

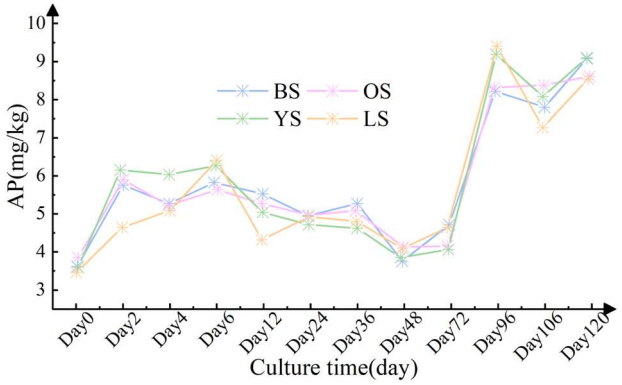

(b) AP

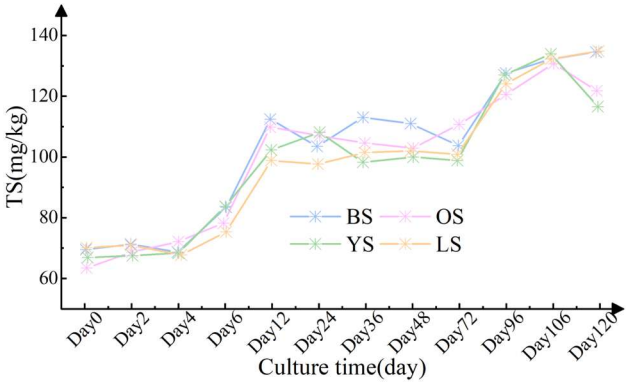

(c) TS

Figure 3: The changes of TN, AP and TS in soil

III. B. 2) Adsorption of mineral ions in soil

Adsorption experiments were conducted using three soil minerals (G, F, M) and three soil mineral-BDOM complexes (GB, FB, MB) as adsorbents, with KH_2PO_4 solution as the phosphorus source. The background electrolyte was selected as 0.02 mol/L KNO_3. Five parallel experiments were conducted, and the average values were taken.

To investigate the role of soil mineral ions in the phosphorus-sulfur cycle, this study explored the adsorption kinetics of phosphorus by soil mineral ions based on the data processing methods outlined in the preceding sections.

Figure 4 shows the adsorption kinetics data of soil mineral ions on phosphorus, where Figures 4(a) and (b) represent the adsorption performance of soil mineral ions and the fitting curves of the pseudo-first-order and pseudo-second-order models, respectively. Table 2 lists the kinetic model parameters of soil mineral-BDOM complexes.

As shown in Figure 4(a), the adsorption process of phosphorus by single minerals and complexes is divided into two stages: a rapid adsorption stage (0–100 min) and a slow adsorption stage (100–4000 min). As time progresses, all adsorbents exhibit this trend. During the initial adsorption phase, due to the presence of sufficient phosphorus adsorption sites on the adsorbent, the adsorption capacity increases rapidly. After entering the slow adsorption stage, the remaining active sites are gradually occupied, and the adsorption reaction gradually reaches equilibrium. After approximately 30 hours, the adsorption capacities of G, GB, F, FB, M, and MB for phosphorus reach 26.03%, 14.64%, 30.95%, 52.48%, 5.71%, and 6.34%, respectively. Based on the basic properties of the adsorbents, it can be seen that FB has the largest specific surface area and pore volume, and the strongest adsorption capacity for phosphorus, while the montmorillonite and MB composite has the weakest. The adsorption performance for phosphorus is ranked from highest to lowest as FB > F > G > GB > MB > M. Experiments have shown that organic matter inhibits the adsorption of phosphorus by goethite, but we found that the combination of BDOM with goethite enhances the mineral's adsorption behavior toward phosphorus. This may be due to the amorphous structure of goethite itself, as well as the selective binding between soil minerals and BDOM. To further analyze the adsorption behavior, the experiments were fitted using pseudo-first-order and pseudo-second-order kinetic models (Figure 4(b)). Based on the fitted adsorption equilibrium capacity and linear relationship data, the quasi-second-order kinetic model better fits the phosphorus adsorption behavior of the soil mineral-BDOM complex (R^2 is closer to 1). This model describes single-layer adsorption dominated by chemical adsorption through electron sharing or exchange, indicating that the adsorption of phosphorus by the soil mineral-BDOM complex is influenced by multiple mechanisms, such as van der Waals forces, π-π interactions, and electrostatic interactions.

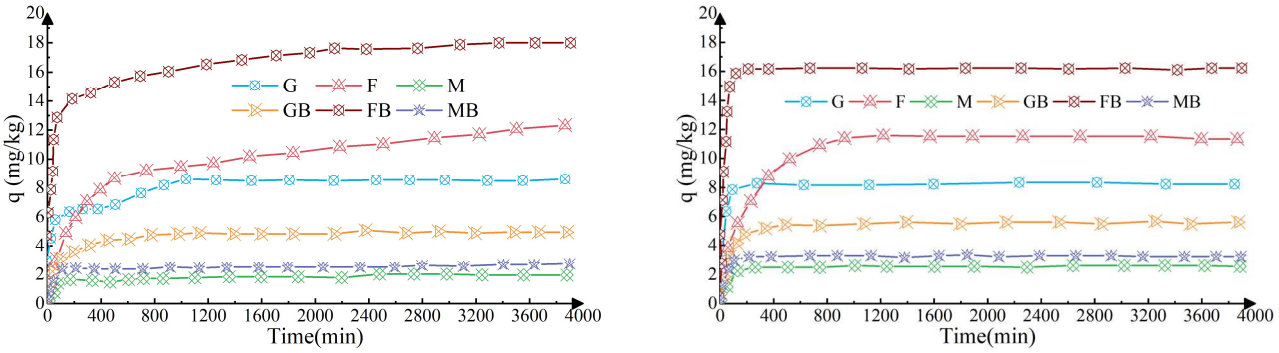

(a) The adsorption performance of soil mineral ions

(b) Quasi - secondary model fitting curve

Figure 4: The adsorption effect of soil mineral ions

Table 2: Dynamic model parameter

Samples	Pseudo-first-order model			Pseudo-second-order model		
	Qe	K_1	R^2	Qe	K_1	R^2
G	6.793	0.043	0.742	7.166	0.011	0.893
F	9.814	0.021	0.931	11.037	0.006	0.967
M	1.563	0.006	0.957	1.638	0.000	0.982
GB	4.208	0.058	0.649	4.426	0.005	0.804
FB	14.172	0.029	0.973	14.826	0.023	0.998
MB	2.004	0.127	0.898	2.096	0.086	0.954

III. C. Key factors influencing the phosphorus-sulfur cycle

III. C. 1) Analysis of the importance of influencing factors

To identify the primary drivers of variations in soil phosphorus and sulfur content, this study utilized the relative change rates of soil mineral ions and microbial activity on phosphorus and sulfur content as response variables. A principal component regression model was employed to conduct a relative importance analysis of various influencing factors related to climatic conditions, field fertilization management, soil properties, biochar application, and its inherent characteristics. The results are presented in Figure 5.

As shown in the figure, among all 16 influencing factors, soil mineral ions are the most significant driving factor for changes in phosphorus and sulfur content, with a relative importance value as high as 31.42%, significantly higher than other influencing factors. The next most significant factors are soil microorganisms (15.06%), soil organic carbon (13.61%), soil total phosphorus (13.42%), soil total nitrogen (12.31%), and biochar application rate (11.25%), annual average temperature (10.37%), and annual average sunshine hours (10.06%), which are all at an overall medium-to-high level, with their respective relative importance values exceeding 10%. The influence of soil mineral ions and microorganisms on changes in phosphorus and sulfur content is least affected by field fertilization management factors (nitrogen-potassium fertilizer ratio, nitrogen-phosphorus fertilizer ratio, and nitrogen fertilizer application rate in inorganic fertilizers), with their relative importance all below 6%.

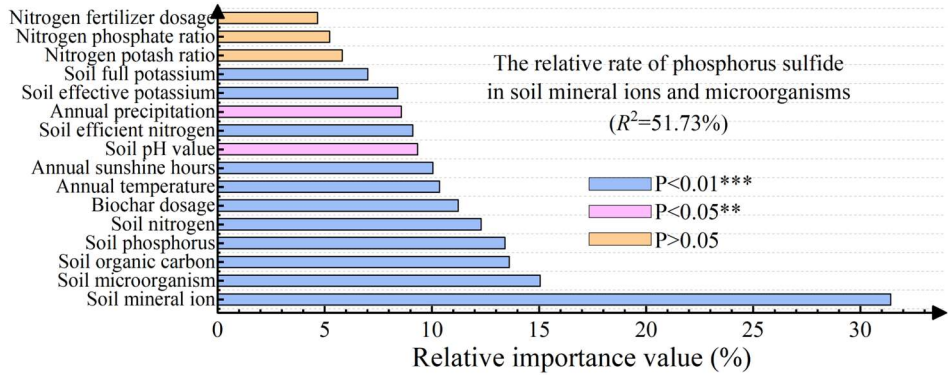

Figure 5: Analysis of the importance of impact factors

Based on the importance analysis of the influencing factors (F1–F16), principal component analysis (PCA) was further applied to reduce the dimensionality, yielding different principal component analysis loadings as shown in Figure 6. As shown in the figure, the cumulative variance contribution rate of the first principal component (PC1) reached 50.38%, primarily comprising soil mineral ions (F1), soil microorganisms (F2), and soil organic carbon (F3). The cumulative variance contribution rate of the second principal component (PC2) is 38.91%, primarily related to soil total phosphorus (F4), soil total nitrogen (F5), biochar application rate (F6), annual average temperature (F7), and annual average sunshine hours (F8). The cumulative variance contribution rates of the first and second principal components combined reached 89.29%, reflecting most of the information on the influence of various factors on soil phosphorus and sulfur cycling. Under the combined influence of the first and second principal components, significant variability exists in soil phosphorus and sulfur cycling.

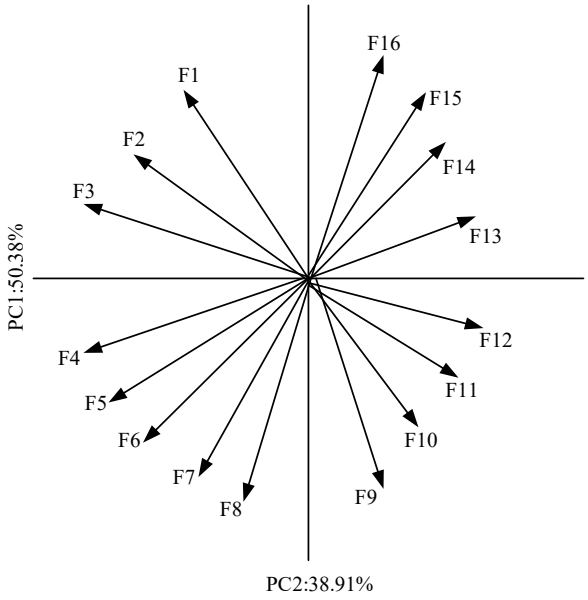

Figure 6: Load diagram of principal component

III. C. 2) Regression analysis of the phosphorus-sulfur cycle

After identifying soil mineral ions and microorganisms as key factors influencing soil phosphorus and sulfur cycling, this study further employed a linear regression model to analyze the specific extent to which extractable mineral ions and microbial content in soil affect phosphorus and sulfur cycling. Figure 7 presents the regression fitting results for phosphorus and sulfur cycling, with Figures 7(a) and 7(b) showing the regression fitting results for soil mineral ions and microorganisms, respectively.

The results of the linear regression analysis indicate that there is a significant positive correlation between phosphorus and sulfur content and mineral ion content in soil ($R^2 = 0.479$, $P < 0.01$), and a positive correlation between phosphorus and sulfur content and microbial abundance in soil ($R^2 = 0.428$, $P < 0.01$). This study found that soil mineral ions significantly increased phosphorus and sulfur content in the soil, and microbial abundance was positively correlated with phosphorus and sulfur content in the soil, which is consistent with the conclusions of existing related studies. Additionally, soil mineral ions significantly increased the calcium and magnesium-bound organic carbon content in soil mineral-bound organic carbon, and the calcium and magnesium-bound organic carbon content was significantly positively correlated with the extractable calcium and magnesium content in the soil. These results indicate that calcium and magnesium ions released by microbial activity can effectively bind with organic carbon molecules in the soil to form calcium and magnesium-bound carbon, revealing another important pathway through which microorganisms promote the formation of mineral-bound organic carbon in soil. Therefore, the interaction between mineral ions and microorganisms in soil significantly enhances phosphorus and sulfur cycling, providing new research directions for enhancing soil fertility and increasing land productivity.

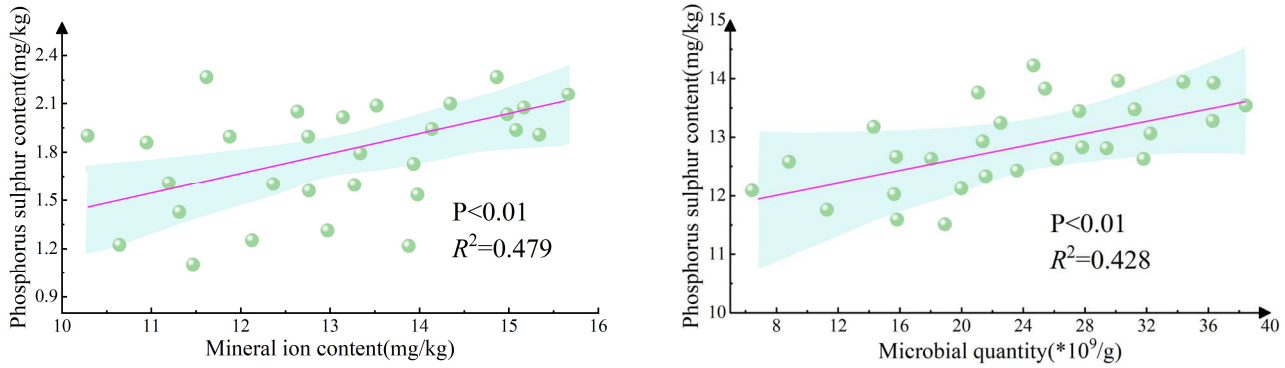

(a) Soil mineral ion (b) Soil microorganism

Figure 7: The regression fitting results of the phosphorus-sulfur cycle

IV. Conclusion

This study selected soil from the experimental base of S Agricultural University as the research subject and employed principal component regression analysis to investigate the specific effects of soil mineral ions and microorganisms on phosphorus-sulfur cycling. The study found that mineral ion complexes in soil enhance phosphorus adsorption, thereby facilitating phosphorus cycling in soil. Additionally, there are significant differences in phosphorus and sulfur cycling among different soil types. Furthermore, the relative importance of mineral ions in soil on phosphorus and sulfur cycling reached 31.42%, and the cumulative variance contribution rate of the first and second principal components in principal component analysis reached 89.29%. Furthermore, soil mineral ions and microbial abundance exert a significant positive influence on phosphorus and sulfur cycling ($P < 0.01$). Therefore, further exploring the changes in soil mineral ions and microorganisms can provide better insights into soil phosphorus and sulfur cycling, offering research guidance for enhancing soil fertility.

References

[1] Wan, X., Yang, J., & Song, W. (2018). Pollution status of agricultural land in China: impact of land use and geographical position. Soil & Water Research, 13(4).

[2] Gomes, E., Inácio, M., Bogdzevič, K., Kalinauskas, M., Karnauskaitė, D., & Pereira, P. (2021). Future land-use changes and its impacts on terrestrial ecosystem services: A review. Science of The Total Environment, 781, 146716.

[3] Zhang, Z., Xie, D., Teng, W., Gu, F., Zhang, R., Cheng, K., ... & Yang, F. (2025). A state of art review on carbon, nitrogen, and phosphorus cycling and efficient utilization in paddy fields. Plant and Soil, 1-21.

[4] Freedman, B., & Baker, N. (2020). Nutrient Cycles. Science, Technology, and Society.

[5] Reinhard, C. T., Planavsky, N. J., Gill, B. C., Ozaki, K., Robbins, L. J., Lyons, T. W., ... & Konhauser, K. O. (2017). Evolution of the global phosphorus cycle. Nature, 541(7637), 386-389.

[6] Zhuang, X., Wang, S., & Wu, S. (2024). Electron transfer in the biogeochemical sulfur cycle. Life, 14(5), 591.
[7] Pacheco, L. P., Monteiro, M. M. D. S., Petter, F. A., Nóbrega, J. C. A., & Santos, A. S. D. (2017). Biomass and nutrient cycling by cover crops in Brazilian Cerrado in the state of Piauí. Revista Caatinga, 30(1), 13-23.
[8] Jiao, S., Chen, W., Wang, J., Du, N., Li, Q., & Wei, G. (2018). Soil microbiomes with distinct assemblies through vertical soil profiles drive the cycling of multiple nutrients in reforested ecosystems. Microbiome, 6, 1-13.
[9] Dai, Z., Xiong, X., Zhu, H., Xu, H., Leng, P., Li, J., ... & Xu, J. (2021). Association of biochar properties with changes in soil bacterial, fungal and fauna communities and nutrient cycling processes. Biochar, 3, 239-254.
[10] Liu, S., Zamanian, K., Schleuss, P. M., Zarebanadkouki, M., & Kuzyakov, Y. (2018). Degradation of Tibetan grasslands: Consequences for carbon and nutrient cycles. Agriculture, Ecosystems & Environment, 252, 93-104.
[11] Helfenstein, J., Tamburini, F., von Sperber, C., Massey, M. S., Pistocchi, C., Chadwick, O. A., ... & Frossard, E. (2018). Combining spectroscopic and isotopic techniques gives a dynamic view of phosphorus cycling in soil. Nature communications, 9(1), 3226.
[12] Zhang, Z., Mao, H., Zhao, Z. Q., Cui, L., Wang, S., & Liu, C. Q. (2021). Sulfur dynamics in forest soil profiles developed on granite under contrasting climate conditions. Science of the Total Environment, 797, 149025.
[13] Chaudhary, S., Sindhu, S. S., Dhanker, R., & Kumari, A. (2023). Microbes-mediated sulphur cycling in soil: Impact on soil fertility, crop production and environmental sustainability. Microbiological Research, 271, 127340.
[14] Hallama, M., Pekrun, C., Lambers, H., & Kandeler, E. (2019). Hidden miners–the roles of cover crops and soil microorganisms in phosphorus cycling through agroecosystems. Plant and soil, 434, 7-45.
[15] Figueroa, I. A., & Coates, J. D. (2017). Microbial phosphite oxidation and its potential role in the global phosphorus and carbon cycles. Advances in Applied Microbiology, 98, 93-117.
[16] Nair, P. R., Kumar, B. M., Nair, V. D., Nair, P. R., Kumar, B. M., & Nair, V. D. (2021). Soil organic matter (SOM) and nutrient cycling. An introduction to agroforestry: Four decades of scientific developments, 383-411.
[17] Geng, Y., Pan, S., Zhang, L., Qiu, J., He, K., Gao, H., ... & Tian, D. (2022). Phosphorus biogeochemistry regulated by carbonates in soil. Environmental Research, 214, 113894.
[18] Tian, J., Ge, F., Zhang, D., Deng, S., & Liu, X. (2021). Roles of phosphate solubilizing microorganisms from managing soil phosphorus deficiency to mediating biogeochemical P cycle. Biology, 10(2), 158.
[19] Wang, S., Yuan, X., Li, T., Yang, J., Zhao, L., Yuan, D., ... & Duan, C. (2024). Changes in soil microbe-mediated carbon, nitrogen and phosphorus cycling during spontaneous succession in abandoned PbZn mining areas. Science of The Total Environment, 920, 171018.
[20] Li, W., Lv, G., & Hu, D. (2022). Soil microbial‐mediated sulfur cycle and ecological network under typical desert halophyte shrubs. Land Degradation & Development, 33(18), 3718-3730.
[21] Saha, B., Saha, S., Padhan, D., Das, A., Poddar, P., Pati, S., & Hazra, G. C. (2019). Sulfur Cycle in Agricultural Soils: Microbiological Aspects. In Biofertilizers and Biopesticides in Sustainable Agriculture (pp. 279-298). Apple Academic Press.
[22] Qi, J., Liu, Y., Wang, Z., Zhao, L., Zhang, W., Wang, Y., & Li, X. (2021). Variations in microbial functional potential associated with phosphorus and sulfur cycling in biological soil crusts of different ages at the Tengger Desert, China. Applied Soil Ecology, 165, 104022.
[23] Chen, M., Luo, Y., Shen, Y., Han, Z., & Cui, Y. (2020). Driving force analysis of irrigation water consumption using principal component regression analysis. Agricultural Water Management, 234, 106089.
[24] Çankaya, S., Eker, S., & Abacı, S. H. (2019). Comparison of Least Squares, Ridge Regression and Principal Component approaches in the presence of multicollinearity in regression analysis. Turkish Journal of Agriculture-Food Science and Technology, 7(8), 1166-1172.
[25] Xu, J., & Hsu, D. J. (2019). On the number of variables to use in principal component regression. Advances in neural information processing systems, 32.